Density functional theory of polydisperse fluid interfaces

Density functional theory of polydisperse fluid interfaces

M Baus[1], L Bellier-Castella[2] and H Xu[2]

[1] Physique des Polymères, Université Libre de Bruxelles, Campus Plaine, CP 223,
B-1050 Brussels, Belgium
[2] Département de Physique des Matériaux (UMR 5586 du CNRS),
Université Claude Bernard-Lyon 1, 69622 Villeurbanne Cedex, France

Abstract
Most colloids usually exhibit one or several polydispersities. A natural framework for the theoretical description of polydisperse systems is provided by the extension of density functional theory to 'continuous' mixtures. This will be illustrated here by the study of both the bulk and interfacial properties of a simple van der Waals model for a polydisperse colloidal fluid.

1. Introduction

Although at present one often uses systems of colloidal particles as experimental prototypes for theoretical models of simple fluids [1], in particular for hard-sphere-like fluids, these systems remain basically complex fluids because the different colloidal particles, while often very similar, are never strictly identical to one another. In order to understand whether a particular experimental feature could be the consequence of this polydispersity of the colloidal particles it is necessary to have at one's disposal a theoretical framework for the analysis of polydisperse systems. The theory of polydisperse fluids, leaving aside some early attempts mainly concerned with polymeric systems [2], can be said to have started two decades ago with the pioneering works of Kincaid [3], Stell [4] and Glandt [5] and their collaborators, soon followed by the pioneering work of Hansen and Barrat [6] on polydisperse colloidal crystals. It seems thus appropriate to dedicate this paper on polydisperse fluid interfaces to Professor Hansen on the occasion of his 60th birthday.

While most of the early papers were concerned with the influence of this polydispersity on a given phase (be it a fluid or a solid phase), many of the more recent papers have tackled various aspects of the study of phase separation in polydisperse fluids [7]. To our knowledge, however, there has been no prior study of the interface between two coexisting polydisperse fluids and it is to this topic that we will dedicate the present study (see [8–10] for technical details).

In section 2 we will generalize the standard density functional theory (DFT) [11] to polydisperse systems. The bulk phase behaviour of a simple polydisperse van der Waals (vdW)

description [8, 9] is summarized in section 3. The corresponding interfacial density and pressure profiles [10] are described in sections 4 and 5, respectively, while the final section 6 contains our conclusions.

2. Density functional theory of polydisperse mixtures

The advantage of DFT over the more traditional statistical mechanical theories [11] results from the fact that its main focus is directly on the average local number density of the different species. This allows one to introduce at an early stage some of the most important structural information about the system to be considered. In a general polydisperse mixture there will be $n = 1, 2, \ldots$ components, each component having a number of attributes, say $\sigma_n^{(s)}$, $s = 1, 2, \ldots$, which were not strictly fixed during its production process (e.g. its form, size and charge) but instead were distributed or dispersed over a finite interval (e.g. $\sigma_{min} < \sigma_n^{(s)} < \sigma_{max}$). For simplicity we only consider here the polydisperse generalization of a simple fluid, i.e. a one-component system of spherical particles with a single polydisperse attribute (e.g. its size). Let then $\rho(\mathbf{r}, \sigma) \, d\mathbf{r} \, d\sigma$ represent the average number of particles whose centre of mass lies within a volume $d\mathbf{r}$ around $\mathbf{r}$ and whose polydisperse attribute σ lies within an interval $d\sigma$ around σ. In what follows it will be convenient to represent this attribute by a dimensionless scalar quantity, σ. We can then associate with the system of average density, $\rho(\mathbf{r}, \sigma)$, a variational free energy, $A([\rho], [\phi])$, which is a functional of $\rho(\mathbf{r}, \sigma)$ (as indicated by the square brackets) and also of the conjugate external field, $\phi(\mathbf{r}, \sigma)$, which acts on $\rho(\mathbf{r}, \sigma)$ so as to produce a system with a given structure. Enlarging now the functional space by this extra σ-dimension, we can extend the usual DFT into

$$A([\rho], [\phi]) = F[\rho] + \int d\sigma \int d\mathbf{r} \, \rho(\mathbf{r}, \sigma)\{\phi(\mathbf{r}, \sigma) - \mu(\sigma)\} \tag{1}$$

where $F[\rho]$ is the density functional:

$$F[\rho] = k_B T \int d\sigma \int d\mathbf{r} \, \rho(\mathbf{r}, \sigma)\{\ln(\rho(\mathbf{r}, \sigma)\Lambda^3(\sigma)) - 1\} + F_{ex}[\rho] \tag{2}$$

of a system of equilibrium temperature T (k_B being Boltzmann's constant), thermal de Broglie wavelength $\Lambda(\sigma)$ (which will depend on the attribute σ whenever the kinetic energy does) and excess free energy $F_{ex}[\rho]$. The equilibrium value of $\rho(\mathbf{r}, \sigma)$ will be given then by the extremum of (1) at fixed $\phi(\mathbf{r}, \sigma)$, i.e. it will be a solution of the following Euler–Lagrange equation:

$$\mu(\sigma) = \phi(\mathbf{r}, \sigma) + k_B T \ln(\rho(\mathbf{r}, \sigma)\Lambda^3(\sigma)) + \frac{\delta F_{ex}[\rho]}{\delta \rho(\mathbf{r}, \sigma)} \tag{3}$$

where $\mu(\sigma)$ is the chemical potential of the 'species' σ. To close equations (1)–(3) and fully specify the system, we need moreover an expression for $F_{ex}[\rho]$. For illustrative purposes we will consider here (having in mind the liquid–vapour interface of spherical particles) a simple vdW expression. In this case $F_{ex}[\rho]$ will consist of a local functional describing the excluded-volume effect due to some hard repulsions and a non-local functional describing the cohesion effect due to some soft attractions, namely,

$$F_{ex}[\rho] = -k_B T \int d\mathbf{r} \int d\sigma \, \rho(\mathbf{r}, \sigma) \ln\left\{1 - \int d\sigma \, v(\sigma)\rho(\mathbf{r}, \sigma)\right\}$$

$$+ \tfrac{1}{2} \int d\mathbf{r} \int d\sigma \int d\mathbf{r}' \int d\sigma' \, \rho(\mathbf{r}, \sigma)V_A(|\mathbf{r} - \mathbf{r}'|; \sigma, \sigma')\rho(\mathbf{r}', \sigma') \tag{4}$$

where $V_A(r; \sigma, \sigma')$ is the pair potential describing the attractions (A) between two particles of species σ and σ', having respective volumes $v(\sigma)$ and $v(\sigma')$. Again, for illustrative
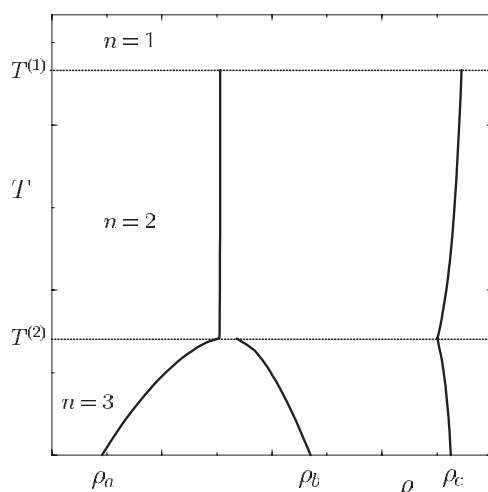
Figure 1. A schematic representation of the one-phase ($n = 1$), two-phase ($n = 2$), three-phase ($n = 3$) etc regions in the temperature–density (T–ρ) plane.

purposes one can use simple polynomial expressions [8] in σ and σ' for $v(\sigma)/v(1)$ and $V_A(r; \sigma, \sigma')/V_A(r; 1, 1)$ where $\sigma = 1$ denotes the reference species used to make σ dimensionless. In the appropriate limits, equation (4) reduces to the well-known expressions used elsewhere for the study of polydisperse bulk phases (namely $\rho(r, \sigma) \to \rho(\sigma)$; cf [8]) or monodisperse interfaces (namely $\rho(r, \sigma) \to \rho(r)\delta(\sigma - 1)$; cf [12]) or monodisperse bulk phases (namely $\rho(r, \sigma) \to \rho\delta(\sigma - 1)$; cf [11, 12]) and we refer the reader to these publications for some of the technical details.

3. Bulk phase coexistence of polydisperse fluids

An interface is a region spatially separating two coexisting bulk phases. Before considering the interface itself it is hence indicated that we should summarize here how the bulk phases are themselves modified by the polydispersity of the system [8]. Let us start from a uniform 'parent' phase of density $\rho(r, \sigma) \to \rho(\sigma) = \rho_0(\sigma)$ and temperature $T = T_0$, where $\rho_0(\sigma)$ is a *given* density distribution fixed by the production process of the parent phase and corresponding to an average density ρ_0, with $\rho_0 = \int d\sigma \, \rho_0(\sigma)$. The quantity $h_0(\sigma) = \rho_0(\sigma)/\rho_0$ describes then how the different σ-values are distributed around the reference value $\sigma = 1$ (usually taken to be the average value of σ in this parent phase) and for simplicity we assume $h_0(\sigma)$ to be singly peaked around $\sigma = 1$. Such a single-peaked or monomodal distribution $h_0(\sigma)$ is appropriate when all the particles are similar (but not identical) and $h_0(\sigma)$ is then usually taken to be of a simple (Gaussian, log-normal, Schulz–Zimm) analytical form [8]. Let α be a measure of the inverse width of $h_0(\sigma)$ such that the monodisperse system is recovered, namely $h_0(\sigma) \to \delta(\sigma - 1)$, when $\alpha \to \infty$ [8]. Let us now consider the vdW model of section 2 and lower T_0, at given ρ_0 and $h_0(\sigma)$, until the system phase separates. Because the polydisperse system can be viewed as a mixture of σ-species with infinitely many components, the Gibbs phase rule allows for phase separation (or fractionation as it is often called here) into two, three, ... phases. Elsewhere [9] we found that the n-phase region is separated from the ($n+1$)-phase region by a well-defined temperature, say $T^{(n)}_{(\alpha)}$, which decreases with increasing n; that is, $T^{(1)}_{(\alpha)} > T^{(2)}_{(\alpha)} > T^{(3)}_{(\alpha)} > \cdots$ (cf figure 1). Note that when $\alpha \to \infty$ the present vdW model has

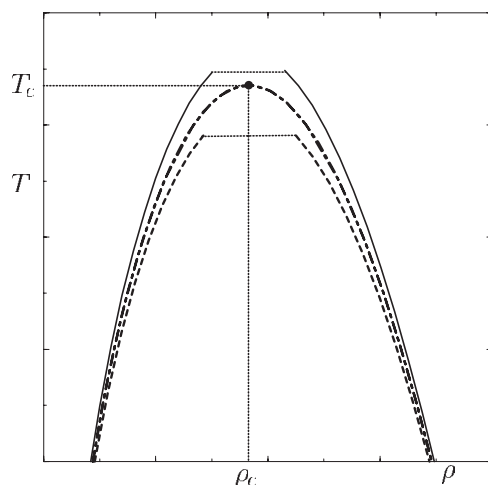**Figure 2.** A schematic representation of a sub-critical ($\rho_0 < \rho_c$, outer curve) and a super-critical ($\rho_0 > \rho_c$, inner curve) binodal around the critical binodal ($\rho = \rho_c$, central curve) passing through the critical point (T_c, ρ_c).

only a one-phase (for $T > T_c$) region, and a two-phase (for $T < T_c$) region, so when $\alpha \to \infty$, all these characteristic temperatures ($T_{(\alpha)}^{(1)}, T_{(\alpha)}^{(2)}, \ldots$) will collapse onto $T_{(\infty)}^{(1)}$. Moreover, when $\alpha \to \infty$ we have $T_{(\infty)}^{(1)} = T_c$, with T_c being the critical-point temperature, whereas for $\alpha \neq \infty$ we find $T_{(\alpha)}^{(1)} > T_c(\alpha)$ (the critical point being defined in each case as the point where the two coexisting phases become identical [8]) with moreover $T_c(\alpha) > T_c(\infty)$. The polydispersity is thus seen to strongly favour phase separation in the system. Let us now lower T_0 from the one-phase ($T_0 > T^{(1)}(\alpha)$) into the two-phase ($T^{(1)}(\alpha) > T_0 > T^{(2)}(\alpha)$) region and compare this two-phase fractionation with the usual vdW liquid–vapour coexistence ($T_c(\infty) > T_0$). If we label the two phases or fractions as 'a' and 'b' with, say, the a-phase being the low-density or 'vapour' phase, we find that the coexisting densities, say ρ_a and ρ_b, depend now both on the temperature *and* on the parent phase density ρ_0—that is $\rho_a(T, \rho_0) < \rho_b(T, \rho_0)$—whereas when $\alpha \to \infty$, the coexisting densities are independent of ρ_0 (only the volume of each phase will depend on ρ_0 via the lever rule). Moreover, each of the coexisting phases or fractions will have a different σ-distribution, say $h_a(\sigma)$ and $h_b(\sigma)$, both of which are different from $h_0(\sigma)$, while their form changes with ρ_0 for a given T, but also with T for a given ρ_0 [8]. Hence, when $\rho_a(T, \rho_0)$ and $\rho_b(T, \rho_0)$ are plotted in the T–ρ plane, there will be a different binodal for each ρ_0 (cf figures 2 and 3). These binodals are moreover truncated upwards at a characteristic temperature $T_m(\rho_0, \alpha)$, except when ρ_0 matches a critical density, $\rho_0 = \rho_c(\alpha)$, in which case the corresponding binodal resembles the usual ($\alpha = \infty$) vdW binodal passing through a critical point $T_c(\alpha)$ (with however $T_c(\alpha) > T_c(\infty)$). When ρ_0 is varied at constant α, the whole set of binodals fills up the space between two limiting curves called the cloud (-point) and shadow curves (intersecting in the critical point).

The complete solution of a phase separation problem is thus much more labour-intensive than that of the corresponding monodisperse ($\alpha = \infty$) system. This has led several authors to content themselves with computing only the cloud and shadow curves and to introduce further approximations to the free energy $F[\rho]$. This however has important drawbacks for e.g. the study of interfacial properties, which requires a knowledge of the binodals. In most applications, $F_{ex}[\rho]$ only depends on a finite number of σ-moments of $\rho(\sigma)$ and this has led some authors [13] to project $F[\rho]$ *a priori* onto these moments while annealing the
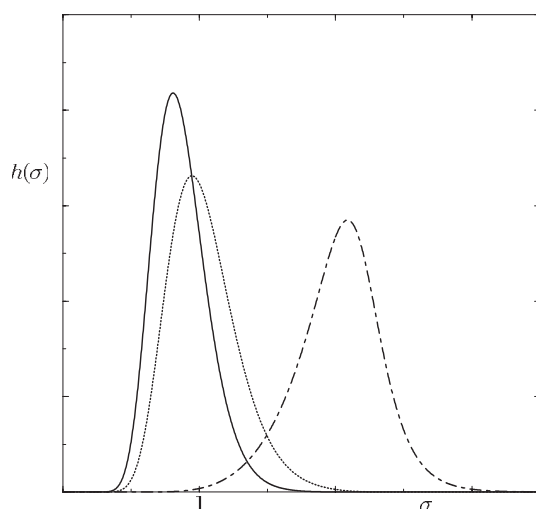
Figure 3. A schematic representation of a parent σ-distribution (central curve) phase separating into a phase enriched in the small-σ species (left curve) and a second phase enriched in the large-σ species (right curve).

remaining moments. This yields a finite-dimensional moment free energy which is easier to handle than the full functional $F[\rho]$ but which also approximates the binodals in an unknown manner. We found it more interesting to project *a posteriori* the integral equation resulting from the full $F[\rho]$ onto these moments because this can be done without approximation and leads to equations which are similar to those of the moment free energy and can hence be solved with the same amount of labour. The really difficult problem which remains concerns the question of the global stability of the solutions, i.e. the construction of the convex envelope to the free-energy functional $F[\rho]$. As shown elsewhere [9], this is indeed a very labour-intensive enterprise even for the simple vdW expression used here.

4. Density profiles and adsorption properties

Let us return now to the interface which separates the two bulk phases. To obtain the density profile across the interface we have to solve now the Euler–Lagrange equation (3) for a two-dimensional density, $\rho(z, \sigma)$, with z being the distance to the planar interface, in such a way that asymptotically ($z \to \pm\infty$) the solution matches the bulk phase density distributions. If $\rho_a(\sigma) = \rho_a h_a(\sigma)$ and $\rho_b(\sigma) = \rho_b h_b(\sigma)$ are the density distributions of the two bulk phases, which, for a given parent phase of density ρ_0 and $h_0(\sigma)$ of inverse width α, are able to coexist, for a T belonging to the two-phase region ($T^{(1)}(\alpha) > T > T^{(2)}(\alpha)$), then the corresponding boundary conditions for the Euler–Lagrange equation will be $\rho(z = \infty, \sigma) = \rho_a(\sigma)$ and $\rho(z = -\infty, \sigma) = \rho_b(\sigma)$. An example of such a density profile, $\rho(z, \sigma)$, is shown in figure 4. The information contained in these profiles can be summarized by calculating the adsorption $\Gamma_1(\sigma)$ of the σ-species at the interface, namely,

$$\Gamma_1(\sigma) = \int_{-\infty}^{\infty} \mathrm{d}z \, (z_1 - z) \rho'(z, \sigma) \tag{5}$$

where $\rho'(z, \sigma) = \partial\rho(z, \sigma)/\partial z$ and $z = z_1$ is the position of the zero-adsorption Gibbs dividing surface of the reference species $\sigma = 1$ (i.e. z_1 is such that $\Gamma_1(\sigma = 1) = 0$). From figure 5 it
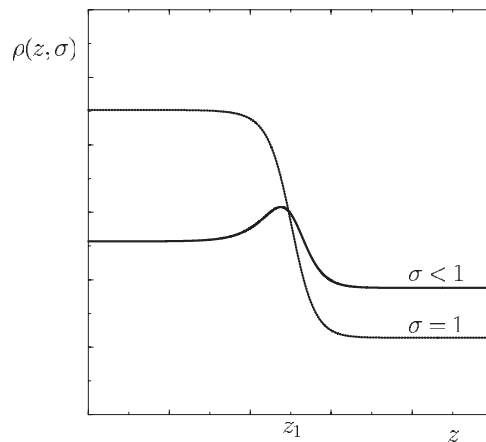
Figure 4. A schematic representation of the density profile of the reference species ($\sigma = 1$) across the interface, and a $\sigma < 1$ species which accumulates in the interfacial region.
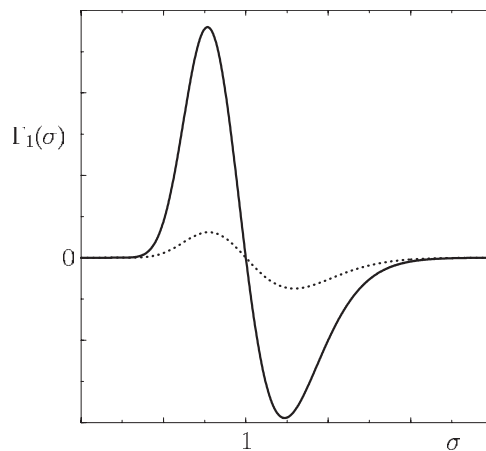

Figure 5. A schematic representation of the rapid variation of the adsorption $\Gamma_1(\sigma)$ with the temperature for a temperature close to critical (dotted curve) and a lower temperature (full curve). Note the excess of the $\sigma < 1$ species and the depletion of the $\sigma > 1$ species, $\Gamma_1(\sigma)$ being referred to the reference species $\sigma = 1$.

is seen that there is a considerable accumulation at the interface of the $\sigma < 1$ species together with a strong depletion of the $\sigma > 1$ species, with an adsorption coefficient $\Gamma_1(\sigma)$ which rapidly increases when the temperature is lowered. The excess of the $\sigma < 1$ species occurs mainly on the low-density side ($z > z_1$) of the interface, while the depletion of the $\sigma > 1$ species is concentrated on its high-density side ($z < z_1$).

5. Pressure profiles and surface tension

Although the pressure is constant in the coexisting bulk phases, there is a pressure deficit in the interfacial region which gives rise there to the interfacial or surface tension [14]. In order to compute this local pressure profile, namely $p(z)$, we divide the two-phase system into two parts separated by a plane perpendicular to the constant-density surfaces. Next we
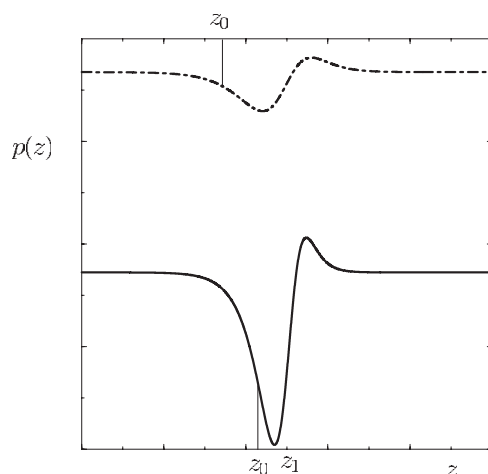
Figure 6. A schematic representation of the pressure profile $p(z)$ across the interface for a temperature close to critical (upper curve) and a lower temperature (lower curve). Note the large pressure deficit on the high-density side and the smaller pressure excess on the low-density side of the interface. The top and bottom z_0 indicate respectively the location of the surface of tension corresponding to the two pressure curves.

infinitesimally deform one part tangentially to the constant-density surfaces and identify the resulting thermodynamic work of deformation with the work of deformation of the pressure forces acting in, and in a direction normal to, the plane separating the two parts [12]. The result is a pressure profile, $p(z)$, which reduces to the constant pressure of the two bulk phases in each bulk phase and which exhibits a profile (namely $p'(z) \neq 0$) in the interfacial region. This profile consists of a large pressure deficit on the high-density side of the interface followed by a smaller pressure excess on the low-density side just as in the monodisperse ($\alpha = \infty$) case, except that here ($\alpha < \infty$) the interfacial region ($p'(z) \neq 0$) is considerably broadened by the polydispersity of the system (cf figure 6). To this pressure profile we can associate a surface tension γ, namely,

$$\gamma = \int_{-\infty}^{\infty} \mathrm{d}z \, (p - p(z)) \equiv \int_{-\infty}^{\infty} \mathrm{d}z \, z p'(z), \tag{6}$$

where $p = p(z = \pm\infty)$ is the bulk pressure, as well as a surface of tension, $z = z_0$:

$$z_0 = \frac{1}{2\gamma} \int_{-\infty}^{\infty} \mathrm{d}z \, z^2 p'(z) \tag{7}$$

with $p'(z) = \mathrm{d}p(z)/\mathrm{d}z$. We find that $z = z_0$ lies on the high-density side ($z_0 < z_1$) of the Gibbs dividing surface, $z = z_1$, of the reference species and that γ vanishes with a classical critical exponent when T approaches $T_c(\alpha)$, as expected for a mean-field vdW theory. More interestingly, we find that $\gamma(\alpha) < \gamma(\alpha = \infty)$ for the low T-values, whereas $\gamma(\alpha) > \gamma(\alpha = \infty)$ when T approaches $T_c(\alpha)$, mainly because $T_c(\alpha) > T_c(\infty)$ (cf figure 7). Both effects are due to the polydispersity, but the influence of the latter is seen here to have a non-monotonic T-dependence.

6. Conclusions

We have shown how DFT, suitably generalized to polydisperse systems, can be used for the study of the interfacial properties of fluid–fluid interfaces of polydisperse systems. The results
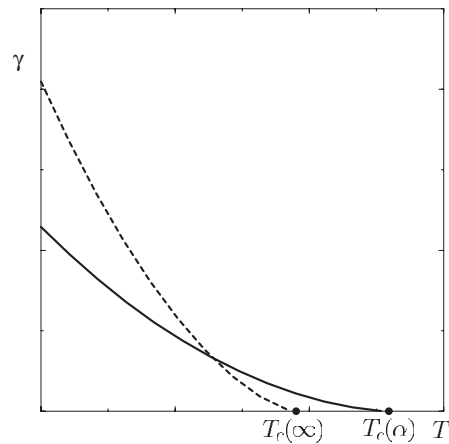
Figure 7. The schematic variation of the surface tension γ with the temperature T for the monodisperse (dashed curve) and the polydisperse (full curve) systems of respective critical temperatures $T_c(\infty)$ and $T_c(\alpha)$.

indicate some interesting differences between the phase behaviour of a polydisperse system and its monodisperse limit studied within the same framework. These results have been obtained from a model free energy but are thought to be fairly robust within the area of the vdW description. Some of the questions analysed here will however be difficult to study by means of computer simulations because the simulation of interfaces requires large systems, the more so when the system is polydisperse. Last but not least, experimental studies will require a careful characterization of the polydispersity of the underlying interaction potential before its results can be analysed within a theoretical framework similar to the one presented here.

Acknowledgment

References

[1] See, e.g.,
Baus M, Rull L F and Ryckaert J P (ed) 1995 *Observation, Prediction and Simulation of Phase Transitions in Complex Fluids* (Dordrecht: Kluwer)
Poon W C K, Pusey P N and Lekkerkerker H N W 1996 *Phys. World* **9**(4) 27
Gast A P and Russel W B 1998 *Phys. Today* **51**(12) 24
[2] Flory P J 1944 *J. Chem. Phys.* **12** 425
Aris R and Gavalas G R 1966 *Phil. Trans. R. Soc.* A **260** 351
[3] Gualtieri J A, Kincaid J M and Morrison G 1982 *J. Chem. Phys.* **77** 521
[4] Salacuse J J and Stell G 1982 *J. Chem. Phys.* **77** 3714
[5] Briano J B and Glandt E D 1984 *J. Chem. Phys.* **80** 3336
[6] Barrat J L and Hansen J-P 1986 *J. Physique* **47** 1547
[7] Sollich P 2002 *J. Phys.: Condens. Matter* **14** R79
Xu H and Baus M 2000 *Phys. Rev.* E **61** 3249
Bartlett P and Warren P B 1999 *Phys. Rev. Lett.* **82** 1979
Warren P B 1999 *Europhys. Lett.* **46** 295
Cuesta J A 1999 *Europhys. Lett.* **46** 197
Evans R M L 1999 *Phys. Rev.* E **59** 3192
Evans R M L, Fairhurst D J and Poon W C K 1998 *Phys. Rev. Lett.* **81** 1326

Warren P B 1998 *Phys. Rev. Lett.* **80** 1369
Sear R P 1998 *Europhys. Lett.* **44** 531
Sollich P and Cates M E 1998 *Phys. Rev. Lett.* **80** 1365 and references therein
[8] Bellier-Castella L, Xu H and Baus M 2000 *J. Chem. Phys.* **113** 8337
[9] Bellier-Castella L, Baus M and Xu H 2001 *J. Chem. Phys.* **115** 3381
[10] Bellier-Castella L, Xu H and Baus M 2002 *Phys. Rev.* E **65** 021503-1
[11] Hansen J-P and McDonald I R 1986 *Theory of Simple Liquids* 2nd edn (London: Academic)
[12] Lovett R and Baus M 1999 *J. Chem. Phys.* **111** 5544
Baus M and Lovett R 1999 *J. Chem. Phys.* **111** 5555
[13] Sollich P, Warren P B and Cates M E 2001 *Adv. Chem. Phys.* **116** 265
[14] Mareschal M, Baus M and Lovett R 1997 *J. Chem. Phys.* **106** 645
El Bardouni H, Mareschal M, Lovett R and Baus M 2000 *J. Chem. Phys.* **113** 9804